

DOI: 10.13745/j.esf.sf.2022.8.33-en

Economic feasibility and efficiency enhancement approaches for in situ upgrading of low-maturity organic-rich shale from an energy consumption ratio perspective

LU Shuangfang^{1,2,3}, WANG Jun³, LI Wenbiao^{1,2,*}, CAO Yixin³, CHEN Fangwen³, LI Jijun³, XUE Haitao³, WANG Min³

1. Sanya Offshore Oil & Gas Research Institute, Northeast Petroleum University, Sanya 572025, China

2. Key Laboratory of Continental Shale Hydrocarbon Accumulation and Efficient Development, Ministry of Education, Northeast Petroleum University, Daqing 163318, China

3. Key Laboratory of Deep Oil and Gas, School of Geosciences, China University of Petroleum (East China), Qingdao 266580, China

Abstract: The technical feasibility of in situ upgrading technology to develop the enormous oil and gas resource potential in low-maturity shale is widely acknowledged. However, because of the large quantities of energy required to heat shale, its economic feasibility is still a matter of debate and has yet to be convincingly demonstrated quantitatively. Based on the energy conservation law, the energy acquisition of oil and gas generation and the energy consumption of organic matter cracking, shale heat-absorption, and surrounding rock heat dissipation during in situ heating were evaluated in this study. The energy consumption ratios for different conditions were determined, and the factors that influence them were analyzed. The results show that the energy consumption ratio increases rapidly with increasing total organic carbon (TOC) content. For oil-prone shales, the TOC content corresponding to an energy consumption ratio of 3 is approximately 4.2%. This indicates that shale with a high TOC content can be expected to reduce the project cost through large-scale operation, making the energy consumption ratio after consideration of the project cost greater than 1. In situ heating and upgrading technology can achieve economic benefits. The main methods for improving the economic feasibility by analyzing factors that influence the energy consumption ratio include the following: (1) exploring technologies that efficiently heat shale but reduce the heat dissipation of surrounding rocks, (2) exploring technologies for efficient transformation of organic matter into oil and gas, i.e., exploring technologies with catalytic effects, or the capability to reduce in situ heating time, and (3) establishing a horizontal well deployment technology that comprehensively considers the energy consumption ratio, time cost, and engineering cost.

Keywords: shale gas content; in situ upgrading; energy consumption ratio; high-efficiency heating; efficient organic matter transformation

1 Introduction

The lacustrine shale of China contains large reserves of oil and gas resources. Therefore, lacustrine shale is a crucial resource that can help alle-

viate the imbalance in the supply and demand of energy in the country^[1-6]. The oil and gas resources of China include immature oil shale that is yet to reach the oil generation threshold, mature “shale oil” in the oil window, and shale gas in highly overmatured shale.

Received: 2022-00-00; Revised: 2022-00-00

Project funding: National Natural Science (Key) Fund Project (Grant Nos. 41972136, 41330313)

First author: Lu Shuangfang, professor, doctoral supervisor; research on unconventional oil and gas geology and oil and gas geochemistry. E-mail: lushuangfang@qq.com

* Corresponding author: Li Wenbiao, doctor; research on shale reservoir evaluation and isotopic effect. E-mail: liwenbiao1996nepu@163.com

Medium- and high-maturity shale oil can be extracted using horizontal shale gas wells and large-scale fracturing technologies. Significant strategic breakthroughs in shale oil extraction have been made in multiple basins^[7-12]. The overall thermal maturity of shale in the terrestrial lacustrine basins of China is significantly lower than that in North America. Except for the Songliao Basin, the burial depth of high-maturity shale with maturity (R_o)=1.3% or above is large (typically > 4500 m). Consequently, the costs of drilling and fracking are high, making them economically infeasible for short-term development. In addition, shale formations in most regions are characterized by high clay mineral contents and low fracturing feasibility. Therefore, the exploitation of shale oil resources using drilling and fracking technologies are limited^[6]. The resource potential of immature shale oil and low- to medium-maturity shale oil is much greater than that of conventional oil and gas^[3,13-15]. However, its extraction is currently possible only by in situ upgrading technology (ISUT)^[3,13]. Therefore, the use of ISUT for the extraction of medium- and low-maturity shale oil and gas has gained significant attention worldwide in recent years^[16-17].

During in situ heating, a large proportion of the macromolecular kerogen and heavy oil containing high non-hydrocarbons and asphaltenes in oil shale is decomposed into lighter oils and gases. The oil and gas contents and gas pressure in the pores, which are the driving forces for production, increase, and the viscosity of the fluid decreases. Therefore, the mobility of oil and gas is greatly enhanced. Simultaneously, heating can cause shale to fracture, resulting in increased permeability, thus aiding the extraction of oil and gas^[3]. There is little disagreement among academic and industrial experts about the technical feasibility of oil and gas extraction using in situ heating technology for oil shale exploration.

The pyrolysis of organic matter is an endothermic reaction that requires a certain amount of thermal energy. During the heating process, various minerals and pore water in the shale formation are also heated, which leads to heat consumption. In addition, some heat is dissipated to the surrounding rock through thermal conduction. Therefore, the

economic feasibility of using ISUT for extracting medium-maturity shale oil has been widely questioned. The concept of using in situ heating technology for oil and gas extraction from oil shale (including shale at the immature stage and low- to medium-maturity stage) was proposed long ago. Many exploratory studies and in situ experiments have been conducted in the United States of America (USA)^[16,18-26]. In China, laboratory simulation experiments and numerical simulations of in situ thermal upgrading have been conducted^[27-37]. However, to the best of our knowledge, there has been no successful commercial application of this technology to date, because of the enormous energy consumption and consequent cost of the heating process, which significantly affect its economic feasibility. Therefore, determining the feasibility of in situ pyrolysis of oil shale to extract shale oil and gas is of great concern to industry experts and policymakers.

The key to the economic feasibility of ISUT is the energy consumption ratio, which is the ratio of the energy of the generated oil and gas to the sum of the energy to heat shale, the equivalent energy of extraction, and the subsequent operational costs. This ratio should be > 1. The extraction and operational costs include the costs of drilling, fracturing, mining, and environmental protection, which are related to many factors, such as the burial depth, well spacing, well diameter, environmental protection, and operational costs. These costs are difficult to assess because of insufficient research data and lack of industry standards and are therefore not considered in this study. However, the energy of the generated oil and gas must be significantly greater than the energy required for heating shale; i.e., the energy consumption ratio, without consideration of operational costs, must be well over 1 (typically, a value ≥ 3 ^[38] is required). Therefore, the extraction costs can be offset through large-scale operation, thereby ensuring the profitability of oil shale resources.

The energy contained in shale oil and gas that is generated by pyrolysis is equal to the energy per unit mass of oil and gas (the calorific value, which can be obtained from reference materials) multiplied by the total amount of the generated oil and gas. The amount of oil and gas is related to the abundance and type of organic matter in

the shale formation. The energy required for shale heating can be divided into the following three components: (1) energy required for the pyrolysis of organic matter, (2) energy consumed by the minerals and pore water in shale during pyrolysis, and (3) energy lost owing to heat dissipation to the surrounding rock.

In this study, based on the energy conservation principle (energy consumption ratio), we evaluated the energy consumption ratio, without considering engineering and operating costs, to determine the basic conditions required for the economic feasibility of in situ heating technology. We then analyzed the effects of other factors on the energy consumption ratio to determine whether the efficiency of the in situ heating method can be improved. We sought in this study to evaluate the economic feasibility of ISUT and possible ways to improve the technology. The results of this study can be used to promote the application of ISUT for optimized oil shale exploitation.

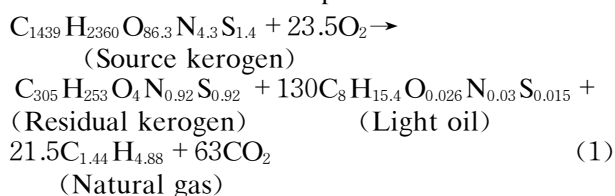
2 Energy consumption ratio of organic matter pyrolysis and oil and gas generation (without consideration of other losses)

2.1 Evaluation of energy consumption by analyzing bond energy difference

The reactant kerogen and reaction products of pyrolysis, including the residual kerogen, oil, gas, and other non-hydrocarbon components, are com-

posed of elements linked by bonds with specific bond energies. Based on the principle of energy conservation, the difference between the bond energies of reactants and products before and after pyrolysis should be the energy required (consumed) for the pyrolysis of organic matter. The calculation process applied in our study was based on Type-I kerogen and is briefly described below.

Using the molecular weight and elemental composition of the source kerogen and residual kerogen provided by Behar et al.^[39] for immature and high-maturity light oil (see Tables 7–11 on page 400 and Figures 7–15 on page 402 in Fu et al.^[40]) and the composition of light oil and natural gas in the high-maturity stage^[41], with CO₂ considered as the main non-hydrocarbon product, the reaction can be expressed as follows:



The number of atoms and bond types in Type-I kerogen and the main reaction products (Table 1-3) can be determined by considering the aromatic carbon content, fatty carbon content, and number of aromatic bonds (C–C, C=C, C=O, O–H, S–S, C–S, C–H, and C–N) in the structural formula in Behar et al.^[39] (see Tables 7–11 on page 400, Tables 7–12 on page 401, and Figures 7–15 on page 402 in Fu et al.^[40]).

Table 1 Atomic number and bond number of Type-I original kerogen, residual kerogen, and other products (modified according to Fu et al.^[40])

Molecular formula and bond type	Number of bonds		
	Source kerogen	Residual kerogen	Light oil molecule
Molecular formula	C ₁₄₃₉ H ₂₃₆₀ O _{86.3} N _{4.3} S _{1.4}	C ₃₀₅ H ₂₅₃ O ₄ N _{0.92} S _{0.92}	C ₈ H _{15.4} O _{0.026} N _{0.03} S _{0.015}
C–C	1251	109	5.975
Benzene-C	40	20	
C=C	4		0.7
C–C triple bond			0.3
Aromatics	96	42	
C–N	12	2	0.03
C–O	263	8	0.03
C=O	78		0.01
C–S	2	2	0.0015
Phenolic hydroxyl C–O	20		
C–H	1770	210	15.32
Benzene-H	80	42	
N–H		1	0.06
Disulfide bond	1		
O–H	65		0.01
S–H			0.0015
Phenol hydroxyl O–H	20		
Total molecular bond energy (kJ/mol)	1604190.18	241314.86	9120.35

Table 2 Composition of wet gas and number of molecular bond types

Molecule type	Proportion/%	Number of C-C	Number of C-H	Total molecular bond energy (kJ/mol)
Methane	70		4	1652.60
Ethane	20	1	6	2816.38
Propane	7	2	8	3980.16
Butane	2	3	10	5143.94
Pentane	1	4	12	6307.72
Total molecular bond energy of wet gas (kJ/mol)				2164.66

Table 3 Number of bond types of other small molecules

Bond type	Carbon dioxide	Oxygen	Nitrogen
O=O		1	
C=O	2		
N-N triple bond			1
Total molecular bond energy (kJ/mol)	1448.38	498.00	946

Based on the bond energy of the various types of molecular bonds (Table 4), we obtained the following results:

Table 4 Dissociation energy of chemical bonds related to structure of kerogen (according to Behar et al.^[39])

Bond type	Dissociation energy (kJ/mol)
C-C	337.48
Benzene-C	380.62
C=C	614.5
C-C triple bond	962.7
Aromatics	2060
C-N	292
C-O	349.58
C=O	723.87
C-S	272
Phenolic hydroxyl C-O	427.6
C-H	413.15
Benzene-H	460
N-H	391
Disulfide bond	268
O-H	463
S-H	339
Phenol hydroxyl O-H	356

Total bond energy of reactants = 1604190.18 (source kerogen) + 23.5 × 498 (oxygen molecules) = 1615893.18 kJ/mol

Total bond energy of products = 241314.86 (residual kerogen) + 130 × 9120.35 (light oil) + 21.5 × 2164.66 (wet gas) + 63 × 2 × 726.22 (carbon dioxide molecules) = 1565004.27 kJ/mol

Difference between the total bond energies of reactants and products = 50888.91 kJ/mol (ΔE). This is the energy consumed in the pyrolysis reaction described by Eq. (1).

It is evident from Eq. (1) that the pyrolysis reaction product contains 130 mol of light oil and 21.5 mol of natural gas. Therefore, the energy required to generate 1 mol of light oil and 0.165 mol of natural gas is 391.45 kJ (50888.91/130).

2.2 Evaluation of energy consumption based on activation energy of hydrocarbon formation (chemical kinetic theory)

Numerous studies on the hydrocarbon generation kinetics of organic matter^[42-43] have shown that the average activation energy required for kerogen-to-oil-and-gas cracking and oil-to-gas cracking ranges from 200 to 260 kJ/mol. Previous studies of the Daqing oil field^[44] have shown that the average activation energies of Type-I kerogen pyrolysis to light oil and natural gas are 209.25 and 226.29 kJ/mol, respectively. Based on these results, the energy required to produce 1 mol of light oil and 0.165 mol of natural gas was estimated to be 246.59 kJ/mol.

Owing to the different rationales behind the two approaches, the energy value based on the activation energy of hydrocarbon formation and that based on the bond energy difference are not entirely consistent. The bond energy conservation method uses an approximate formula, because the kerogen structure, composition, and hydrocarbon formation process are extremely complex and change constantly, which makes it impossible to represent the chemical reaction accurately. Moreover, the bond energy is approximated be-

cause the bond energy can be affected by the surrounding groups; therefore, the values given by different reference materials differ. In the activation energy method, the energy required to produce non-hydrocarbon products is not considered. Nevertheless, the calculated values for the thermal energy required to produce 1 mol of light oil obtained based on these two methods are relatively close and range from 246 to 391 kJ/mol. Therefore, the evaluation results obtained with these two methods can be considered mutually corroborative.

2.3 Energy consumption ratio of oil and gas generated by heating to pyrolysis heat consumption (without considering other losses)

Based on previous studies^[45-46], the amounts of heat (average calorific values) generated by the combustion of 1 mol of light oil and 0.165 mol of natural gas (methane) were calculated as 7233.84 and 146.90 kJ (890.3×0.165), respectively, and the total calorific value was calculated as 7380.74 kJ.

Based on the calorific value (7380.74 kJ/mol) of hydrocarbons (1 mol of oil + 0.165 mol of gas) generated in the pyrolysis reaction and the heat required for cracking organic matter to oil and gas (246.59 – 391.45 kJ/mol), the energy consumption ratio considering only the generation of oil and gas was calculated to range from 18.9 to 29.9. Thus, ISUT is economically feasible if we consider only the energy consumed during pyrolysis. Notably, further evaluation is required to consider the effects of heat absorption by inorganic minerals and water and heat dissipation to the surrounding rock.

3 Energy consumption in shale heating process because of heat absorption and dissipation

The amount of heat absorbed by the inorganic minerals and water in shale is related to the heating temperature (field) and thermal capacity of the shale. Heat energy consumption due to dissipation from shale to the surrounding rock is controlled by the temperature field, the thermal

conductivity of the surrounding rock, and the conduction duration. The distribution of the temperature field in a shale formation is related to the temperature and location of the heat source, the spacing between the heating and production wells, the thickness and thermal conductivity of the formation, and the heating duration. Therefore, a geological model is required for quantitative evaluation.

3.1 Geological model and parameters

In the stratigraphic model of an electric heating system for a horizontal well shown in Figure 1, h is the shale formation thickness, and L is the horizontal length of the heating well. Production and heating wells were equal in length and deployed in parallel, with d representing the distance between the two wells. As shown in Figure 1, the horizontal wells were set in the middle of the shale formation. The starting point of the heating well was set as the coordinate system origin ($x = 0$, $y = 0$, and $z = 0$), with x being the transverse direction between the heating and production wells, y being the vertical direction, and z being the direction along the horizontal well.

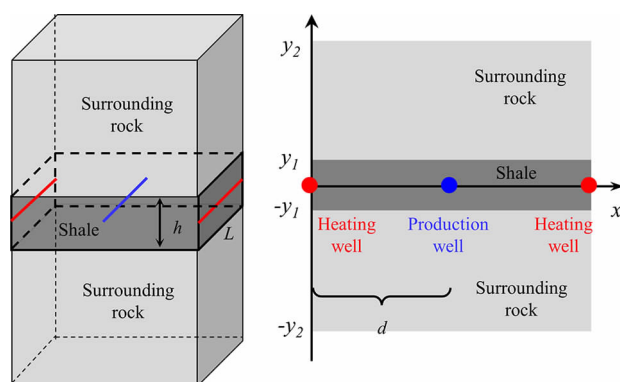


Fig.1 Stratigraphic model of horizontal well system (heating and production wells)

Values for the thermal conductivity, thermal capacity, and density of the shale formation required for the numerical simulation were obtained from existing literature^[47-50]. The values of other simulation parameters were selected based on geological conditions or according to the simulation requirements (Table 5).

Table 5 Relevant parameters for simulation developed in this study

Model parameter	Parameter value	Model parameter	Parameter value
Shale/sandstone length (m)	Sufficient	Shale thermal conductivity (W/m/K)	1.0–2.4 (1.21)
Shale thickness (m)	30	Surrounding rock thermal conductivity (W/m/K)	2.1–3.5 (3)
Sandstone thickness (m)	500	Shale specific heat (J/kg/K)	1100–2000 (1141)
Wellbore radius (m)	0.02/0.05/0.1/0.2/0.5	Specific heat of surrounding rock /(J/kg/K)	762–1071.8 (890)
Well spacing (m)	5/10/15/20/25	Shale density (kg/m ³)	2100–2800 (2450)
Burial depth of the bottom of shale layer (m)	1800	Density of surrounding rock /(kg/m ³)	1800–2800 (2470)
Ground surface temperature (°C)	20	Heating well temperature (°C)	500/600/700/800/900
TOC (%)	1–20 (5)	Production well temperature (°C)	200/250/300/350/400
HI (mgHC/gTOC)	800	Geothermal gradient (°C/m)	0.033

Note: 5/10/15/20/25 are several values of the same parameter in the model; 1–20 (5) represents a range of values, with 5 being the parameter value selected for the model

3.2 Thermal conductivity equations and initial and boundary conditions

The general form of the three-dimensional thermal conductivity equation is as follows^[51]:

$$\frac{\partial T_i(x, y, z, t)}{\partial t} = \frac{k_i}{c_i \rho_i} \left(\frac{\partial^2 T_i}{\partial x^2} + \frac{\partial^2 T_i}{\partial y^2} + \frac{\partial^2 T_i}{\partial z^2} \right) \quad (2)$$

where, when $i = 1$ (i.e., $-y_1 < y < y_1$), the equation is used to describe the thermal conductivity of the shale formation, and when $i = 2$ (i.e., $y_1 < y < y_2$ or $-y_2 < y < -y_1$), the equation is used to describe the thermal conductivity of the surrounding rock formation.

The initial conditions were determined using the following equations from the geological model:

$$T(t = 0) = T_{\text{res}}(H) \quad (3)$$

where $T_{\text{res}}(H)$ is the shale formation temperature before heating, which is set as the original ground temperature, considering the geothermal gradient (°C).

The boundary conditions are as follows:

$$T(x^2 + y^2 \leq r_{\text{well}}^2, t) = T_{\text{heat}} \quad (4)$$

where r_{well} is the wellbore diameter (m) and T_{heat} is the temperature of the heat source of the heating well (°C).

$$\frac{\partial T}{\partial t}(x = 0, y, t) = \frac{\partial T}{\partial t}(x = 2d, y, t) = 0 \quad (5)$$

(Note: owing to the symmetry of the geological model, as shown in Figure 1, no heat passes through the formation faces parallel to the heating well.)

$$\frac{\partial T}{\partial t}(x, y = y_2, t) = \frac{\partial T}{\partial t}(x, y = -y_2, t) = 0 \quad (6)$$

(Note: when the thickness of the surrounding rock is sufficiently large, the artificial heating

field will not affect the temperatures at the top and bottom boundaries.)

Thus, the interface condition is expressed as follows:

$$T_1(x, y = \pm y_1, t) = T_2(x, y = \pm y_1, t) \quad (7)$$

(Note: the temperatures at the top and bottom interfaces between shale and the surrounding rock will be the same; $+y_1$ and $-y_1$ represent the top and bottom interfaces, respectively.)

$$k_1 \frac{\partial T_1}{\partial t} \Big|_{y = \pm y_1} = k_2 \frac{\partial T_2}{\partial t} \Big|_{y = \pm y_1} \quad (8)$$

(Note: the heat fluxes at the top and bottom interfaces between shale and the surrounding rock will be the same; $+y_1$ and $-y_1$ represent the top and bottom shale interfaces, respectively.)

3.3 Temperature field determination

The thermal conductivity equation (Eq.(2)) and the initial, boundary, and interface conditions (Eqs.(3–8)), as well as the relevant parameters listed in Table 5, were used to calculate the temperature $T(x, y, z, \text{ and } t)$ at any point $(x, y, \text{ and } z)$ at time t ; the temperature field of the shale formation was obtained thereby. Figure 2a illustrates the temperature field of the shale formation model shown in Figure 1 for a formation thickness (h) of 30 m, well spacing (d) of 5 m, heating source temperature (T_{heat}) of 700 °C; the production well was heated to a temperature of 300 °C. Figure 2b illustrates the temperature-time history of four representative points in the shale formation. The results indicate that the time required to heat the production well (Point 3) to a temperature of 300 °C is 4.05 years when the well spacing is 5 m, at which time the tem-

perature at Point 1 at the edge of the shale formation is only 110 °C. Thus, it is evident that the heat conduction process in shale formations is extremely slow.

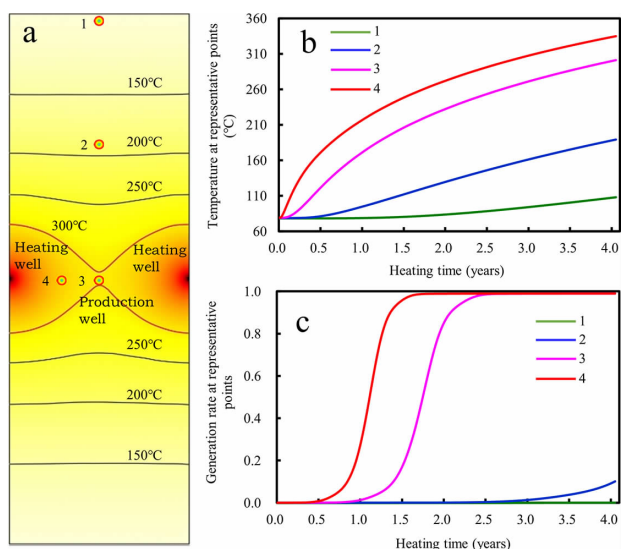


Fig.2 (a) Calculated temperature field of shale formation; (b) thermal history; and (c) hydrocarbon generation rates at representative points

3.4 Evaluation of energy gain during the heating process

Based on the temperature-time history at any point at any time $T(x, y, z, \text{ and } t)$ obtained as described in the previous section (Figure 2b), we used the chemical kinetic model of hydrocarbon generation from organic matter to calculate the hydrocarbon generation rate $XH(x, y, z, \text{ and } t)$ as follows:

$$XH(x, y, z, t) = \sum_{i=1}^{NH} XH_i = \sum_{i=1}^{NH} XH_{i0} \left\{ 1 - \exp \left[- \int_0^t AH_i \exp \left(- \frac{EH_i}{RT} \right) dt \right] \right\} \quad (9)$$

where XH is the generation rate of hydrocarbon from kerogen, NH is the number of parallel reactions of kerogen-to-hydrocarbon conversion, EH_i is the activation energy corresponding to each reaction, AH_i is the pre-exponential factor, and XH_{i0} ($i = 1, 2, \dots, NH$) is the hydrocarbon potential of the source kerogen in each reaction. It is also possible to calculate the oil or gas generation rate separately from kerogen by replacing H in Eq.(9) with O or G , respectively, which represents the conversion rate of kerogen to oil or gas, respectively. Owing to space limitations,

the derivation process is not presented in this manuscript. Interested readers can refer to the authors' previous work^[41,43-44].

Thermal history data for the four representative points shown in Figure 2a were substituted into Eq.(9) to obtain the evolution of the hydrocarbon generation rate at each point with respect to the heating time (Figure 2c). The results indicated that the production well (Point 3) and a point closer to the heating well (Point 4) reached a temperature of approximately 260 °C in 2.5 years and 1.7 years, respectively, at which time the hydrocarbon generation rate was close to 1. Point 2, which was farther from the heating well, required 4.05 years to reach a temperature of 185 °C, at which time the hydrocarbon conversion had just begun, and the generation rate was approximately 10%. At the edge of the shale formation (Point 1), the temperature did not reach 110 °C, and the hydrocarbon conversion process did not occur at a significant scale.

The thermal energy (q_i) of the shale volume conversion into oil and gas corresponding to a given point based on the hydrocarbon generation rate at that point is expressed as follows:

$$q_i = \rho_s \times dv_i \times \text{TOC} \times HI \times \left(\frac{XO(x, y, z, t)}{M_o} \times q_o + \frac{XG(x, y, z, t)}{M_g} \times q_g \right) \quad (10)$$

where ρ_s is the shale formation density (kg/m³), dv_i is the shale volume at point i (m³), TOC content is the total organic carbon content of shale, HI is the hydrocarbon potential of the organic matter, XO is the oil generation rate, q_o is the calorific value of oil per molar mass unit (J/mol), q_g is the calorific value of gas per molar mass unit (J/mol), M_o is the molar mass of light oil (kg/mol), and M_g is the molar mass of natural gas (kg/mol). The parameter values required for the calculation are listed in Table 3.

The total energy gain, Q_1 , was obtained by summing (integrating) the potential energy of the shale volume between the heating well and the production well, as shown in Figure 2.

$$Q_1 = \iiint q_i \quad (11)$$

3.5 Evaluation of energy consumption during heating

(1) Kerogen-bond dissociation energy, Q_2 :

The total (integral) energy consumption required to break all kerogen bonds between the heating well and the production well can be expressed as follows:

$$Q_2 = \iiint \frac{\rho_s}{M_k} \times q_k \times \frac{\text{TOC}}{0.84} \times XH(x,y,z) dv \quad (12)$$

where M_k is the molar mass of kerogen (kg/mol), q_k is the bond dissociation energy required for kerogen per unit molar mass (J/mol), and 0.84 is the conversion coefficient between TOC and kerogen.

(2) Heat absorption of shale minerals, Q_3 :

The total (integral) heat absorption of the shale formation between the heating and production wells from the initial temperature field to the final temperature field is expressed using the following equation:

$$Q_3 = c_s \rho_s \iiint [T_s - T_{s0}] dv_s \quad (13)$$

where c_s is the thermal capacity of shale (J/kg · K), ρ_s is the density of the shale formation (kg/m³), T_{s0} is the temperature at a given point before heating (K), and T_s is the temperature at that point after heating (K).

(3) The heat absorbed by the surrounding rock formation (heat dissipation due to thermal conduction), Q_4 , is expressed by the following equation:

$$Q_4 = c_w \rho_w \iiint [T_w - T_{w0}] dv_w \quad (14)$$

where c_w is the thermal capacity of the surrounding rock (J/kg · K), ρ_w is the density of the surrounding rock formation (K), T_{w0} is the temperature at a given point before heating (K), and T_w is the temperature at that point after heating (K).

3.6 Energy consumption ratio (R) during heating

According to the foregoing quantitative evaluation process, the energy consumption ratio based on a specific parameter can be expressed by the following equation:

$$R = \frac{Q_1 \times \gamma}{Q_2 + Q_3 + Q_4} \quad (15)$$

where γ is the recovery rate. The oil and gas produced after heating are characterized by the light oil quality, high gas/oil ratio, and high recovery rate. The value of γ was assumed to be 75% in this study.

Figure 3 illustrates the relationship between the energy consumption ratio and TOC content for different heat source temperatures (other parameters are listed in Table 5). It is evident that the heat source temperature has a small impact on the energy consumption ratio, whereas the TOC content of the shale formation has a significant effect on the energy consumption ratio. This is expected because the energy gain increases in proportion to the TOC content (Eq.10). However, the energy consumption due to heat absorption by shale and the surrounding rock formation remains unchanged, and only the energy consumption of kerogen pyrolysis increases. As shown in Figure 3, when the energy consumption ratio is 1, the corresponding TOC content is approximately 1.1%. When the TOC content is below this value, the pyrolysis energy consumption exceeds the energy generated by the oil and gas, and the process is not economically profitable, because the engineering cost and recovery rate are not considered. When the energy consumption ratio is 3, the corresponding TOC content is approximately 4.2%, which indicates that the engineering costs can be offset through large-scale operations when the TOC content is approximately 4%. Therefore, the energy consumption ratio after considering the engineering costs is > 1 , and ISUT is considered to be economically feasible. Therefore, the energy consumption ratio increases with the TOC content. When the TOC content is 18%, the energy consumption ratio is as high as 7; in such a case, there is room for further development of ISUT to identify more economically feasible means of oil shale exploration.

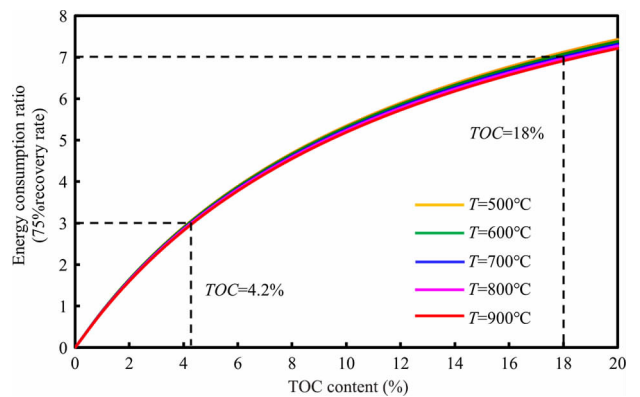


Fig.3 Relationship between energy consumption ratio and TOC content under different heat source temperatures

For example, the shale in the Chang 7 Member of the Ordos Basin has a thickness of >100 m at the center of the lake basin. The TOC content of the shale ranges from 2% to 28%, with an average of 11.7%. The TOC content of more than 80% of the shale samples exceeds 5%. Based on these considerations, it is economically feasible to develop Ordos Chang 7 shale through ISUT.

4 Factors affecting energy consumption ratio and methods to increase efficiency

4.1 Effect of well spacing and methods to improve efficiency

The effect of well spacing on the energy consumption ratio was evaluated using the method described previously, as illustrated in Figure 4a. The energy consumption ratio is the highest when the horizontal well spacing is half the thickness of the shale formation. If the well spacing increases or decreases from this value, the energy consumption ratio decreases. This is because the unnecessary heat dissipation to the surrounding rock formation is 2.08 times the heat consumption of the shale formation when the well spacing is significantly greater than the half-thickness of the shale formation, such as 25 m, as shown in Figure 4b. This is because the upper and lower boundaries of the shale formation also typically reach a higher temperature when the shale around the production well reaches the effective cracking temperature. This results in the dissipation of a considerable amount of heat to the surrounding rocks, which inevitably reduces the energy consumption ratio. However, if the well spacing is less than half the thickness of the shale formation, the temperatures at the top and bottom boundaries of the shale formation remain relatively low when the production well temperature reaches the temperature required for a high hydrocarbon generation rate. In such a case, when the heat dissipation to the surrounding rock formation is low, the temperature at the edges of the shale formation is also low. For example, when the well spacing is 5 m, the heat dissipation to the surrounding rock and the energy consumption of the shale formation is practically negligible, at approximately 0.04. Consequently, the

organic matter at the edges of the shale formation may not have started to crack effectively; therefore, the energy consumption ratio is also relatively low (Figure 4b). In addition, a small well spacing requires a high drilling density, which increases the drilling cost; this is not conducive to improving the economic feasibility of the engineering operation.

As shown in Figure 4c, the production well requires a long time to reach 200 °C owing to the low heat conduction rate of shale; organic matter then begins to crack at a high rate. When the well spacing is 5 m, the time required for the organic matter to crack is 2.4 years; similarly, when the well spacing is 25 m, the required time exceeds 66.4 years. Furthermore, when the well spacing is 15 m and the energy consumption rate is relatively high, the required time is 23.7 years. Therefore, the time cost due to thermal conductivity is enormously high. This is due to the low heat conduction efficiency of shale. Therefore, exploring effective ways to improve the heating efficiency is a crucial to increasing the overall efficiency of ISUT.

The shale heating methods currently being tested in laboratories and mines worldwide can be categorized into four types: electric (resistance), convection heating, microwave/electromagnetic wave, and self-heating (exothermic reaction-based heating) methods^[16,27,32-33,52-53]. (1) The advantages of electric heating are that it has a simple principle, equipment cost is low, and it is a relatively mature technology. However, this method relies on thermal conductivity; therefore, the heating rate is low, and heat loss due to heat dissipation is substantial (Figure 4). Therefore, the potential to improve its efficiency is very low. In the convection heating method, after a group of wells is connected through fracturing, the heating and production wells can be mutually converted to allow uniform heating of the shale formation. This is done based on the convection of high-heat fluid and the heat conduction of shale. In theory, there is a notable reduction in heat conduction distance, thereby improving the heating efficiency. Therefore, this method has the potential to improve efficiency. (2) From the laboratory perspective, microwave

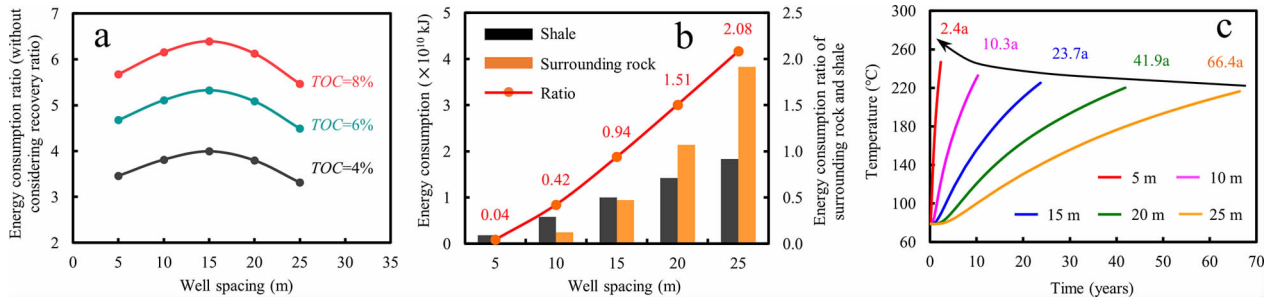


Fig.4 Influence of well spacing on energy consumption ratio: the relationship between well spacing and (a) energy consumption rate; (b) energy consumption of the surrounding rock/shale formations; and (c) heating time and temperature.

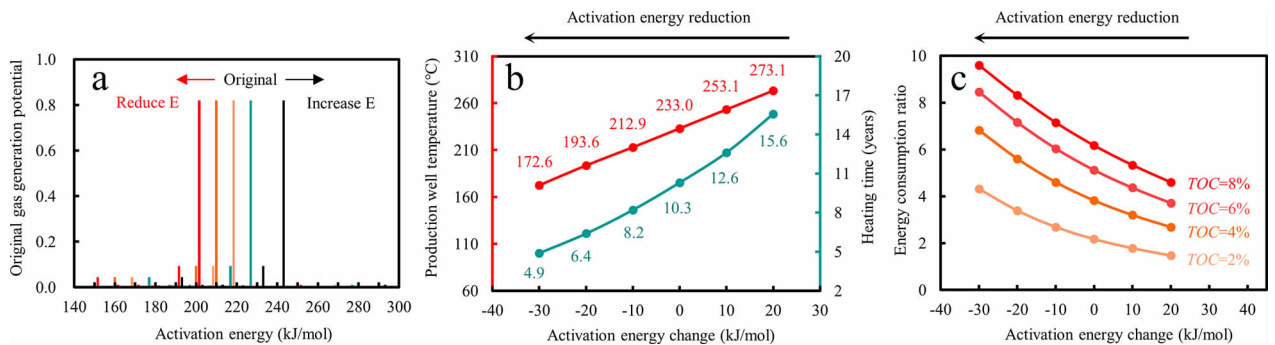


Fig.5 Influence of catalytic effect (activation energy E) on energy consumption ratio

heating allows instantaneous volumetric heating with high heating speed, low heat dissipation, and high thermal efficiency. Therefore, this method has a high potential to improve efficiency. However, direct microwave heating is characterized by low penetration depth. Which means that, the heating process still relies on the low-efficiency heat conduction of shale beyond the penetration depth. Hence, novel technical solutions to increase the penetration depth should be explored. In addition, further studies are needed on the use of microwave equipment smaller than the well diameter to propagate electromagnetic waves into the shale formation efficiently. (3) In the self-heating method, the shale formation is heated by the energy generated via the combustion of organic matter. The efficiency of this method could potentially be improved by utilizing the organic matter present in the shale formation. However, further studies should be conducted on novel methods to initiate the reaction at fixed points and carry out the experiment in a controllable and efficient manner when the organic matter is dispersed. Although the latter three technologies are not as mature as the elec-

tric heating technology, they are worth exploring because they have the potential to overcome the challenge of inefficient heat conduction in shale.

4.2 Impact of catalytic effect (activation energy for hydrocarbon generation) on energy consumption ratio and ways to improve efficiency

By changing the activation energy in Eq.(9) while keeping other conditions/parameters fixed (Figure 5a), we simulated the temperature, time (Figure 5b), and corresponding energy consumption rate (Figure 5c) required for the effective cracking of organic matter in the production well. The results showed that the temperature required for effective pyrolysis of organic matter in the production well decreased from 273.1 to 172.6 °C, the heating time decreased from 15.6 to 4.9 years, and there was a notable improvement in the energy consumption ratio as the activation energy decreased. This was because a lower activation energy of hydrocarbon generation leads to a lower temperature and a shorter time required for the effective pyrolysis of kerogen. Therefore, the energy consumption through heat absorption and conduction by the shale formation is reduced, and a higher energy consumption ratio is achieved.

An effective method for reducing the activation energy of the pyrolysis reaction is by adding catalysts. Therefore, exploring catalytic effect-based technologies to improve the efficiency of hydrocarbon generation from organic matter is one of the most effective ways to improve the overall efficiency of ISUT. Moreover, this would be difficult to achieve using electric heating methods; however, fluid convection and exothermic reaction methods have the potential to carry catalysts by means of fracturing fluids. Neto et al.^[54] showed that when oil shale is heated with microwaves, the temperature required for pyrolysis was reduced by 80 °C in comparison to the conventional heating temperature (380 °C). In addition, the temperature required for pyrolysis was reduced to 245 °C after the addition of a 5% acidic molecular sieve catalyst. These results suggest that the electromagnetic wave heating method may have a catalytic effect and thus require less energy input and a lower temperature to achieve the same results as conventional heating methods.

Among the four heating technologies described above, the latter three have the potential for improved efficiency because of their catalytic effect.

4.3 Effect of heat source temperature

As shown in Figure 6, when the heat source temperature increased from 500 to 900 °C, the full-cracking time of organic matter in the production well shortened (corresponding to a slight increase in temperature). Thus, using a high-temperature heat source can save time and reduce costs. However, increasing the temperature of the heat source produced a high-temperature field near the heating well, which led to increased energy consumption by the inorganic

minerals and a slight, albeit relatively insignificant, decrease in the energy consumption ratio (Figure 3). Therefore, we concluded that the overall effect of heat source temperature on the heating efficiency is small.

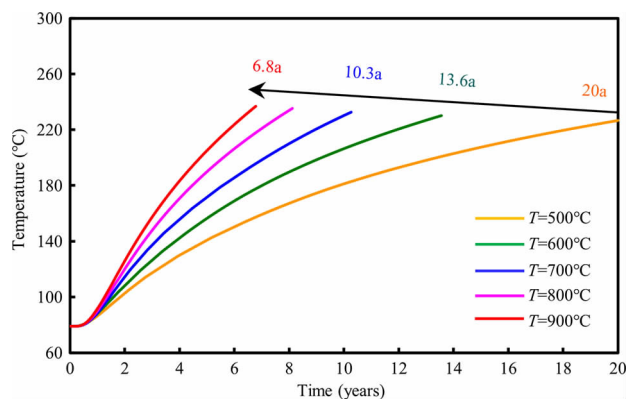


Fig.6 Effect of heat source temperature on heating well

4.4 Effect of heating cable radius

Figure 7 illustrates the effect of heating cable radius on the heating time (Figure 7a) and energy consumption ratio (Figure 7b). The results indicated that a larger heating cable radius leads to a larger area of heat transfer and a shorter heating time, which can reduce the time cost significantly while reducing the energy consumption ratio. However, large heating wells are generally not cost-effective when considering the high cost of drilling bore wells.

4.5 Effect of well layout

Figure 8 illustrates the effect of the well layout on the heating effect. It is evident that when a dual-well layout of horizontal (mode H-1) and vertical wells (mode V-1) is used with the same well spacing (half the shale formation thickness, 15 m), the energy consumption ratios of the horizontal wells are considerably higher than those of the vertical wells. This is because the heat source is

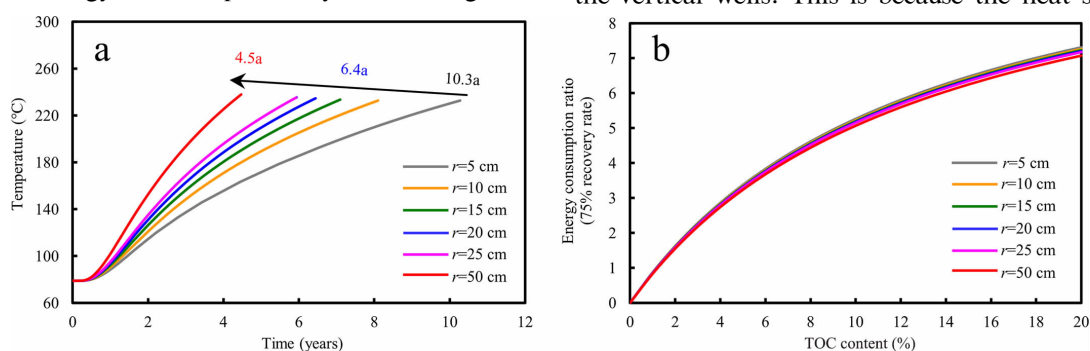


Fig.7 Effect of heating cable radius r (heating well diameter)

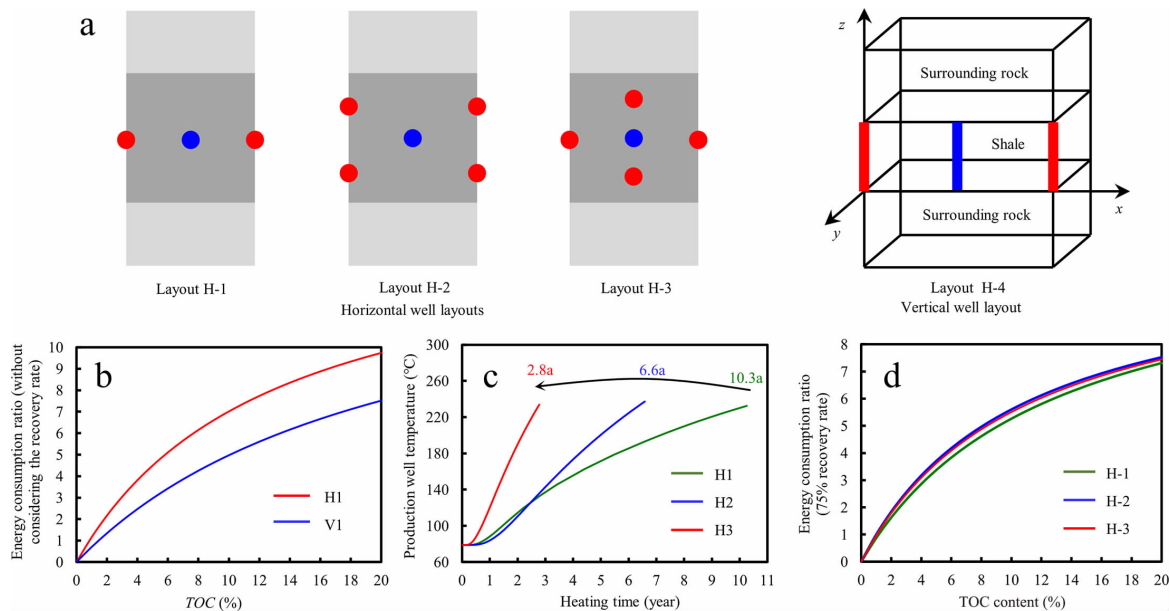


Fig.8 Impact of well layout on heating effect, according to different modes; (a) well layout mode (red, heating well; blue, production well); (b) horizontal well vs. vertical well; (c) heating time of horizontal wells for different modes; and (d) energy consumption ratio of horizontal wells for different modes

placed in the shale formation when horizontal wells were used; this heats the shale formation, and heat dissipates into the surrounding rock only after the thermal conduction reaches the upper and lower boundaries of the shale formation. In contrast, the heat is dissipated into the surrounding rock from the onset of the heating process when vertical wells are used.

The heating times and energy consumption ratios differed for the various layouts of horizontal wells when the horizontal spacing was 15 m. It is evident from Figure 8c that the time required for heating the production well to the temperature required for complete cracking (96%) of organic matter is 10.3 years when the double-well layout (H-1) is used. The heating time for the four-well layouts is considerably shorter, i.e., 6.6 and 2.8 years for the H-2 and H-3 layouts, respectively. These results can be attributed to the higher number of heat sources and the consequent increase in heat supply intensity. In addition, the higher heating rate in the H-3 layout was related to the shorter spacing between the upper and lower heating wells and the intermediate production well. In terms of the energy consumption ratio, multiple-well layouts yield slightly better results, with the H-3 layout having a slightly lower ratio than the H-2 layout. This is related to the fact that the upper and lower heating wells in the

H-3 layout are closer to the shale formation boundary; therefore, more heat dissipates into the surrounding rock. Overall, the use of multi-well layouts improves the energy consumption ratio and significantly reduces the time cost, but increases the drilling cost. Therefore, it is necessary to comprehensively consider the energy consumption ratio and time and engineering costs and quantitatively determine an overall optimization plan.

4.6 Effect of model dimensions on heating

Figure 9 illustrates the effect of model dimensionality on the effectiveness of shale heating. The one-dimensional conduction model appears to have the most effective heating process. For example, when the well spacing (d) is 10 m, the production well reaches a temperature of 300 °C in 2.0 years, and in the two- and three-dimensional models, the heating process requires 20.5 and 190 years, respectively (Figure 9). This is because the one-dimensional model ignores heat conduction in other dimensions, i.e., no heat diffusion occurs, as if thermal insulation conditions exist. This unreasonable assumption is often used in numerical simulations of in situ heating operations^[55]. The thermal efficiency of shale formation is often significantly overestimated because the heat dissipation in other dimensions is neglected. The assumptions of the two-dimensional conduction model are reasonable in specific situations. For

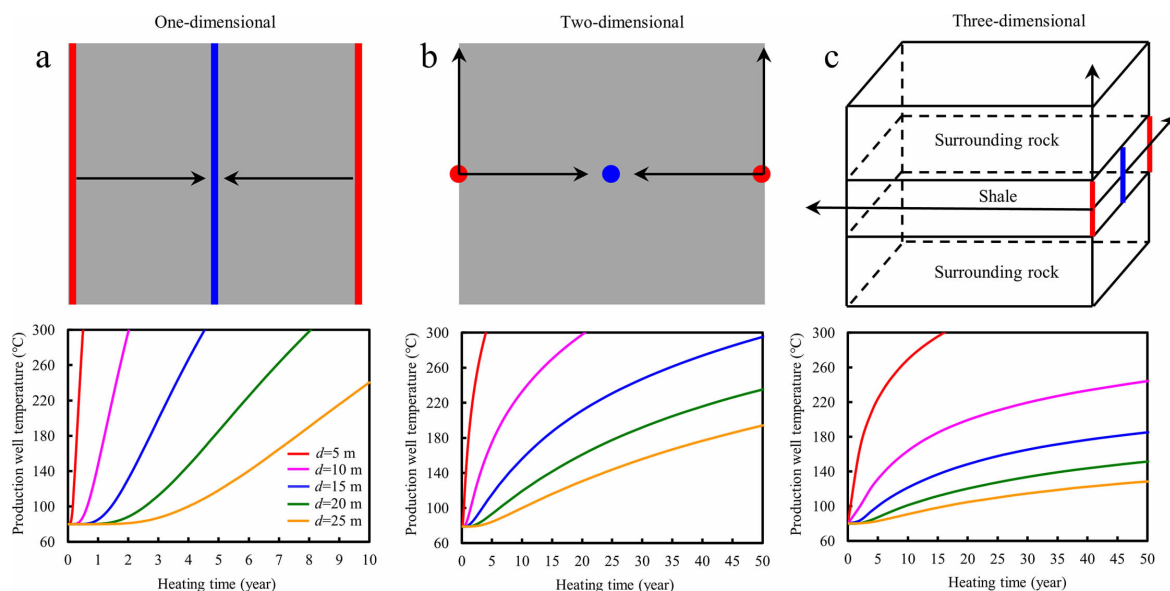


Fig.9 Effect of model dimensions on heating

example, when the horizontal well section is long, the heat conduction along the shaft direction can be ignored to a certain extent. However, in layouts with vertical wells, the heat dissipation along the well axis direction (toward the surrounding rock) cannot be neglected because the length of the well section is typically short; therefore, a corresponding three-dimensional model must be established to accurately characterize the heat dissipation in this type of well layout.

5 Conclusion

In this study, we presented a quantitative evaluation of ISUT of oil shale from the perspective of the energy conservation principle. The results are as follows:

(1) Energy gain from the oil and gas produced by pyrolysis was approximately 18.9–29.9 times the energy consumed during the pyrolysis of organic matter (energy consumption ratio). This confirms that this technology may be economically feasible. After considering the effect of heat absorption by the inorganic components of shale and heat dissipation to the surrounding rock, the energy consumption ratio increased with TOC content. Under certain conditions, the TOC content corresponding to the energy consumption ratio of 1 is approximately 1.1%, and when the TOC is lower than this value, the energy consumption of the pyrolysis process exceeds

the energy gain of the generated oil and gas; thus, the process is economically infeasible. When the energy consumption ratio is 3, the corresponding TOC content is approximately 4.2%, which indicates that the project costs can be offset through large-scale operation when the TOC content exceeds this value. Thus, the energy consumption ratio after considering the engineering costs should be >1 . Under these conditions, ISUT can be economically feasible. Notably, a higher TOC content results in a higher energy consumption ratio; for example, when TOC content = 18%, the energy consumption ratio is as high as 7. In such instances, it would be more beneficial to explore different technical approaches to improve the economic feasibility of the method.

(2) The well layout has a significant impact on the energy consumption ratio. When other conditions were similar, the energy consumption ratio of the horizontal well was significantly higher than that of the vertical well. Therefore, the horizontal well layout was the preferred layout when using ISUT. The multi-well layout only slightly increased the energy consumption ratio and significantly reduced the time cost; however, it significantly increased the drilling cost. Therefore, the energy consumption ratio and time and engineering costs must be considered while quantitatively evaluating novel methods for improving the economic feasibility of ISUT. Overall, it can be concluded that a reasonable layout

of heating and production wells can improve the efficiency of the technology.

(3) The energy consumption ratio was the highest when the horizontal well spacing was half the thickness of the shale formation. The energy consumption ratio was lower when the horizontal well spacing was smaller or greater than half the shale formation thickness. A well spacing that is too large can lead to increased heat dissipation to the surrounding rock formation, and a well spacing that is too small can result in insufficient heating of the shale formation boundaries, while increasing the drilling costs. The electric heating technology has a very high time cost because of the poor heat conduction of shale and the consequent low heating efficiency. Therefore, the second important way to increase the efficiency of ISUT is to explore alternative heating technologies such as convection and electromagnetic heating methods.

(4) Catalytic effects can effectively reduce the temperature and time cost of the pyrolysis reaction while reducing the energy consumption due to heat absorption by shale and heat dissipation to the surrounding rock. This leads to an increase in the energy consumption ratio. Therefore, the third important way to increase the efficiency of ISUT is to explore the use of non-electric heating technologies with catalytic effects to improve the efficiency of hydrocarbon generation from organic matter.

References

- [1] ZOU C N, TAO S Z, HOU L H. Unconventional Petroleum Geology[M]. Beijing: Geological Publishing House, 2014.
- [2] JIA C Z, ZOU C N, YANG Z. Significant progress of continental petroleum geology theory in basins of Central and Western China[J]. Petroleum Exploration and Development, 2018, 45(4): 546-560.
- [3] ZHAI W Z, HU S Y, HOU L H, et al. Connotation and strategic role of in-situ conversion processing of shale oil underground in the onshore China[J]. Petroleum Exploration and Development, 2018, 45(4): 537-545.
- [4] LU S F, HUANG W B, CHEN F W, et al. Classification and evaluation criteria of shale oil and gas resources: discussion and application[J]. Petroleum Exploration and Development, 2012, 39(2): 249-255.
- [5] LU S F, XUE H T, WANG M. Several key issues and research trends in evaluation of shale oil[J]. Acta Petrolei Sinica, 2016, 37(10): 1309-1322.
- [6] LU S F, XUE H T. Formation conditions, occurrence mechanism and enrichment distribution of shale oil[M]. Beijing: Petroleum Industry Press, 2021.
- [7] CHEN X, WANG M, YAN Y X, et al. Continental shale oil exploration[M]. Beijing: Petroleum Industry Press, 2015.
- [8] LIU B, LV Y F, MENG Y L, et al. Petrologic characteristics and genetic model of lacustrine lamellar fine-grained rock and its significance for shale oil exploration: A case study of Permian Lucaogou Formation in Malang sag, Santanghu Basin, NW China[J]. Petroleum Exploration and Development, 2015, 42(5): 598-607.
- [9] ZHAO X Z, ZHOU L H, PU X G, et al. Geological characteristics of shale rock system and shale oil exploration breakthrough in a lacustrine basin: A case study from the Paleogene 1st sub-member of Kong 2 Member in Cangdong sag, Bohai Bay Basin, China[J]. Petroleum Exploration and Development, 2018, 45(3): 361-372.
- [10] ZHI D M, TANG Y, YANG Z F, et al. Geological characteristics and accumulation mechanism of continental shale oil in Jimusaer sag, Junggar Basin[J]. Oil & Gas Geology, 2019, 40(3): 524-534.
- [11] FU J H, LIU X Y, LI S X, et al. Discovery and resource potential of shale oil of Chang 7 member, Triassic Yanchang Formation, Ordos Basin[J]. China Petroleum Exploration, 2021, 26(5): 1-11.
- [12] HE W Y, MENG Q A, FENG Z H, et al. In-situ accumulation theory and exploration & development practice of Gulong shale oil in Songliao Basin[J]. Acta Petrolei Sinica, 2022, 43(1): 1-14.
- [13] ZHANG Y Q. "Small Targets" for Natural Gas[J]. Energy Review, 2017(2): 1.
- [14] LIU Z J, LIU R. Oil shale resource state and evaluating system[J]. Earth Science Frontiers (China University of Geoscience, Beijing; Peking University), 2005(3): 315-323.
- [15] LI S Y, TANG X, HE J L, et al. Global oil shale development and utilization today: two oil shale symposiums held in 2012[J]. Sino-Global Energy, 2013, 18(1): 3-11.
- [16] CUI J W, ZHU R K, HOU L H, et al. Shale in-situ mining technology status quo of challenges and opportunities[J]. Unconventional oil & gas, 2018, 5(6): 103-114.
- [17] YANG Z, ZOU C N, FU J H, et al. Selection of pilot areas for testing in-situ conversion/upgrading processing in lacustrine shale: a case study of Yanchang-7 member in Ordos Basin[J]. Journal of Shenzhen University Science and Engineering, 2017, 34(3): 221-228.
- [18] WALL E T. Method and apparatus for recovering carbon products from oil shale: US[P]. 1983.
- [19] BARTIS J T, LATOURRETTE T, DIXON L, et al. Oil shale development in the United States: prospects and policy issues[R]. Santa Monica, CA: The RAND corporation, 2005.
- [20] HAROLD. Harold Vinegar Shell's in-situ conversion process [R]. Colorado; 26th Oil Shale Symposium, 2006.
- [21] FOWLER T D, VINEGAR H J. Oil shale ICP - Colorado field pilots[R]. San Jose: SPE Western Regional Meeting, 2009.
- [22] LEVERETTE H M. Status and plans for the U.S. department of interior program for development of oil shale and oil sands[R]. Colorado; 31th Oil Shale Symposium, 2011.

- [23] TANAKA P L, YEAKEL J D, SYMINGTON W A, et al. Plan to test ExxonMobil's in situ oil shale technology on a propose RD&A lease[R]. Colorado: 31th Oil Shale Symposium, 2011.
- [24] MARK D L. Chevron's plans for rubblization of Green River Formation oil shale (Gros) for chemical conversion [R]. Colorado: 31th Oil Shale Symposium, 2011.
- [25] ALAN B. Initial results from the AMOSO RD&D pilot test program[R]. Colorado: 32th Oil Shale Symposium, 2012.
- [26] WANG Y P, WANG Y W, MENG X L, et al. Enlightenment of American's oil shale in-situ retorting technology [J]. Oil Drilling & Production Technology, 2013, 35(6): 55-59.
- [27] KANG Z Q, ZHAO Y S, YANG D, et al. Physical principle and numerical analysis of oil shale development using in-situ conversion process technology[J]. Acta Petrolei Sinica, 2008(4): 592-595.
- [28] YANG D, ZHAO J, KANG Z Q, et al. Technology and numerical analysis of in-situ electrical heating on oil shale [J]. Journal of Liaoning Technical University (Natural Science), 2010, 29(3): 365-368.
- [29] WANG Q W. Experimental on thermal and electrical physical properties of oil shale in Jilin Huadian area[D]. Changchun: Jilin University, 2011.
- [30] WANG Q, ZHANG L, BAI J R, et al. The influence of microwave drying on physicochemical properties of Liushuhe oil shale[J]. Oil Shale, 2011, 28: 29-41.
- [31] WANG Q, GU Z Y, BAI J R, et al. Comparative study of the characteristics of oil shale with hot air drying and microwave drying[J]. Energy Procedia, 2012, 17: 884-891.
- [32] ZHAO L. Experimental study on in-situ mining based over-heat steam convection heating oil shale [D]. Taiyuan: Taiyuan University Of Technology, 2015.
- [33] XIA T. Research on in-situ electrical heating development of oil shale reservoir by numerical simulation[D]. Qingdao: China University of Petroleum (East China), 2015.
- [34] XUE J X, LIU Z H. Numerical simulation of the temperature field distribution of oil shale under in-situ process by the electricity heating method[J]. Chinese Journal of Underground Space and Engineering, 2015, 11(3): 669-672.
- [35] WANG Y D, WANG X Y, XING Y F, et al. Three-dimensional numerical simulation of enhancing shale gas desorption by electrical heating with horizontal wells [J]. Journal of Natural Gas Science and Engineering, 2017, 38: 94-106.
- [36] WU Y B, WANG H Z, JIANG Y W. Well pattern optimization for in-situ conversion process in shale oil reservoirs [C]. IFEDC-20182137, Xi'an: Shanxi Petroleum Society, 2018: 955-963.
- [37] ZHANG B, YU C, CUI J W. Kinetic simulation of hydrocarbon generation and its application to in-situ conversion of shale oil[J]. Petroleum Exploration and Development, 2019, 46(6): 1212-1219.
- [38] Haibei Energy. 15 E&P technologies affecting the future of the oil and gas industry[EB/OL]. <https://mp.weixin.qq.com/s/jYp8ikVYo4DtSTeIoUr66A>, 2019-1-18.
- [39] BEHAR F, VANDENBROUCKE M. Chemical modelling of kerogens[J]. Organic Geochemistry, 1987, 11(1): 15-24.
- [40] FU J M, QIN K Z. Kerogen Geochemistry[M]. Guangdong: Guangdong Science and Technology Press, 1995: 373-436.
- [41] LU S F, ZHANG M. Oil and Gas Geochemistry[M]. Beijing: Petroleum Industry Press, 2018: 1-316.
- [42] UNGERER P. State of the art of research in kinetic modeling of oil formation and expulsion[J]. Organic Geochemistry, 1990, 16(1): 1-25.
- [43] LU S F. Theory and Application of hydrocarbon formation kinetics of organic matter[M]. Beijing: Petroleum Industry Press, 1996: 1-199.
- [44] LU S F, LI D, WANG Y W, et al. Resource evaluation method for generating condensate oil and light oil from sapropelic organic matter and its application[J]. Acta Petrolei Sinica, 2007, 28(5): 63-67.
- [45] XING Q Y, PEI W W, XU R Q, et al. Basic Organic Chemistry (I)[M]. Beijing: Higher Education Press, 2005: 1-598.
- [46] WANG Q, ZHANG Y, CHI M S. Pyrolysis properties of kerogen and the determination of aliphatic content of chain [J]. Acta Petrolei Sinica (Petroleum processing section), 2017, 33(4): 771-776.
- [47] WANG T F, LU S X, ZHU Y J. Study on the thermal properties of Chinese oil shale II. The measurement of specific heat of oil shale, char and spent shale[J]. Journal of Fuel Chemistry and Technology, 1987(4): 311-316.
- [48] ZHOU K, SUN Y H, LI Q, et al. Experimenta; research about thermogravimetric analysis and thermal physical properties of Nong'an oil shale[J]. Global Geology, 2016, 35(4): 1178-1184.
- [49] CUI J W, HOU L H, ZHU R K, et al. Thermal conductivity properties of rocks in the Chang 7 SHALE STRATA IN THE Ordos Basin and its implications for shale oil in-situ development[J]. Petroleum Geology & Experiment, 2019, 41(2): 280-288.
- [50] Ministry of Construction of the People's Republic of China, General Administration of Quality Supervision, Inspection and Quarantine of the People's Republic of China. GB 50366—2005 Technical code for ground-source heat pump system[S]. Beijing: China Construction Industry Press, 2009: 11-30.
- [51] SNEDDON IN. Fourier transforms[M]. Princeton: Princeton University Press, 1950: 1-542.
- [52] WANG S P, LIU D X, WANG H H, et al. Current situation and development potential of electric heating process of in-situ oil shale conversion[J]. Natural Gas Industry, 2011, 31(2): 114-118.
- [53] LIU D X, WANG H Y, ZHENG D W, et al. World progress of oil shale in-situ exploitation methods[J]. Natural Gas Industry, 2009, 29(5): 128-132.
- [54] NETO A, THOMAS S, BOND G, et al. The oil shale transformation in the presence of an acidic BEA zeolite under microwave irradiation[J]. Energy & Fuels, 2014, 28(4): 2365-2377.
- [55] WU M. The study of electric heating on hydrocarbon generation and pores evolution of shale in North Songliao Basin [D]. Qingdao: China University of Petroleum (East China), 2020.